J. Fluid Mech. (1985), *vol.* 150, *pp.* 441–450
Printed in Great Britain

Some observations of the subcritical transition in plane Poiseuille flow

By MICHIO NISHIOKA AND MASAHITO ASAI
College of Engineering, University of Osaka Prefecture, Sakai, Osaka, Japan

(Received 16 April 1984)

The subcritical transition in plane Poiseuille flow (generated in a long wind channel of rectangular cross-section) was studied experimentally. Cylinder-generated vortical disturbances were introduced into the parabolic flow (in the test section) or the inlet flow. The parabolic flow was also disturbed by a controlled periodic jet from a wall orifice. On the basis of the three kinds of observations, we come to the conclusion that the minimum transition Reynolds number is about 1000 and the related threshold intensity (of the external disturbance triggering the transition) is comparable to the maximum intensity of u-fluctuations in fully turbulent channel flows.

1. Introduction

Since most duct flows in various engineering systems can undergo laminar-to-turbulent transition below the critical Reynolds number for the linear instability, it is of practical importance to understand and predict the subcritical transition. This rests on our full understanding of the subcritical instability with respect to finite-amplitude disturbances. The subcritical instability has been intensively studied mainly on plane Poiseuille flow since the great theoretical step made by Meksyn & Stuart (1951) and Stuart (1960). The theoretical and experimental progress in this subject has been reviewed in detail by Herbert (1981), Morkovin (1983) and Diprima & Stuart (1983), and only a brief review is given here. Experimentally, plane Poiseuille flow can be generated in a long channel of rectangular cross-section with a large width-to-depth (aspect) ratio. Throughout this paper the Reynolds number R is defined using the centreline velocity U_c, the channel half-depth h and the kinematic viscosity ν.

Some important experimental studies on the transition of plane Poiseuille flow were first made by Davies & White (1928) using a water channel of aspect ratio larger than 37. They disturbed the flow by a right-angled corner at the channel inlet. The present authors believe that the corner caused flow separation. Indeed the wall-pressure measurements indicated inlet disturbances for $R > 150$. The transition Reynolds number found was about 1080. Using a wind channel of aspect ratio 48, Patel & Head (1969) obtained almost the same transition Reynolds number of about 1035. The inlet flow was disturbed by right-angled corners as in Davies & White's experiments. These transition Reynolds numbers are less than 20 % of the critical Reynolds number (5772) for the linear instability (Orszag 1971). The transition in these experiments was caused by high-intensity disturbances in the inlet flow. If disturbances are weak and the channel is of finite length, the parabolic flow can remain laminar even beyond the critical Reynolds number, as shown by Nishioka, Iida & Ichikawa (1975) and Kozlov & Ramazanov (1980).

Meksyn & Stuart (1951) first estimated the nonlinear critical Reynolds number for

two-dimensional disturbances to be about 2900. Zahn *et al.* (1974) and Herbert (1976) obtained almost the same value of about 2700–2900. However, these values are much larger than the transition Reynolds number observed by Davies & White. To examine effects of three-dimensional disturbances on the subcritical transition, Orszag and coworkers conducted numerical simulations. In particular, Orszag & Patera (1983) found that the parabolic flow modified by the two-dimensional wave motion (of the Orr–Sommerfeld mode) is extremely unstable to infinitesimal three-dimensional disturbances when the wave amplitude is above a threshold. They emphasized the three-dimensional linear instability (with the threshold behaviour) as a key mechanism of the subcritical transition and termed it the secondary instability. Subsequently Herbert (1983) showed that the heart of the secondary instability is a kind of parametric resonance. The critical Reynolds number for the secondary instability was estimated by Orszag & Patera to be about 1000. The threshold was about $0.2U_c$ (r.m.s. value), which is larger than the maximum u-fluctuations (13–15% of U_c) in fully turbulent channel flows. Because of the arbitrary choice of the two-dimensional wave, their simulations do not correspond directly to any experiments available, though this does not invalidate the important concept of the secondary instability.

Recently, Carlson, Widnall & Peeters (1982) made a beautiful flow-visualization study of the transition in a water-channel of aspect ratio of 133. They reported that the channel was carefully constructed with a smooth contraction in order to achieve a low-turbulence background flow. Although they did not measure the background turbulence, we may suppose that the intensity was much smaller than that of Davies & White or Patel & Head. Nevertheless, turbulent spots (or patches) appeared spontaneously, leading to a transition at R slightly above 1000 as in Davies & White. The observations by Carlson *et al.* suggest that disturbances that can trigger the transition at R about 1000 need not be so large as the maximum intensity in fully turbulent channel flows.

Since no previous experimental studies reported any data for the intensity of the disturbances triggering the transition at the cited minimum Reynolds number, we decided to obtain some knowledge on this point.

2. Experimental procedure

The experiments are carried out in a rectangular wind channel of aspect ratio 27.4. The width, depth and length are respectively 400, 14.6 and 6000 mm. The half-depth h, on which the Reynolds number is defined, is 7.3 mm. The flow, generated by a Sirocco fan, is passed through five damping screens (of 100 mesh) spanning across both the diffuser section and the settling chamber, and then contracted smoothly into the channel inlet; the contraction ratio is 27.4. The mean velocity U and the fluctuation u in the streamwise direction are measured by linearized hot-wire anemometers. In the test section, which extends beyond $550h$ from the inlet, the velocity distribution across the depth is parabolic, with background turbulence less than 0.05% of U_c. The parabolic flow remains laminar for Reynolds numbers up to 8000, beyond which turbulent bursts occur spontaneously. Even under such low-turbulence conditions, the flow would not remain laminar above the critical Reynolds number for the linear instability (5772) if the channel length were infinite. The wind channel is the same as described in Nishioka *et al.* (1975), except that a damping screen (at the furthest-downstream section) in the settling chamber was replaced. The newly installed screen (of the same nominal mesh size as the original) changed the original pattern of the slight distortion of parabolic flow and increased the degree of the

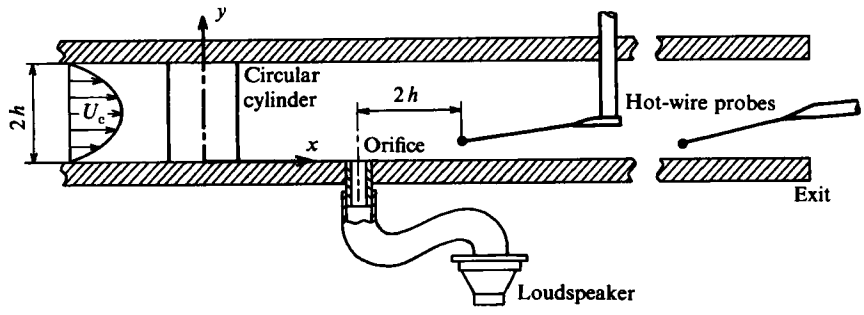

FIGURE 1. Schematic diagram of test section (not to scale). The half-depth h is 7.3 mm. A circular cylinder (10 mm in diameter) is used to disturb the parabolic flow. The flow can be also disturbed by a periodic jet from a wall orifice of 2.7 mm, which is driven by a loudspeaker (10 cm woofer).

three-dimensionality. The three-dimensionality appears only for Reynolds numbers above 3000, below which the flow is almost perfectly two-dimensional.

In order to disturb significantly the laminar flow in the test section we used a circular cylinder of diameter 10 mm, which is larger than the half-depth $h = 7.3$ mm (see figure 1). The cylinder was chosen because it can generate strong disturbances independently of the Reynolds number in the range of our interest. Spanning across the full depth with its axis normal to the walls, the cylinder introduces three-dimensional steady and unsteady vortical disturbances into the otherwise two-dimensional parabolic flow. Local shear layers separate from the cylinder surface and evolve into structures not unlike the Kármán vortex. As they travel downstream, these vortex structures undergo tilting and stretching to produce and enhance the vorticity components in various directions. The flow also separates from the channel walls around the cylinder. This results in the formation of so-called horseshoe vortices. Thus the cylinder-generated disturbance is of high intensity and rich in flow structures. When we observed the transition under disturbed inlet conditions, six cylinders of the same diameter (10 mm) were used. The arrangement will be described later.

In order to examine the threshold nature of the subcritical transition minutely, the parabolic flow was disturbed by a periodic jet from a small wall orifice. Its diameter 2.7 mm is 37 % of the half-depth h. The jet was driven by a loudspeaker. The apparatus was originally used by Nishioka *et al.* (1980) to study the secondary high-frequency instability in the ribbon-induced transition at $R = 5000$. The hot-wire probe in the test section has a vertical stem of diameter 3 mm, which can generate disturbances in the wake. The probe was taken out so as not to introduce the additional disturbances when we observed the jet-induced transition at the channel exit.

3. Results and discussion

We first describe the cylinder-generated disturbance at $R = 900$. The cylinder was placed at the spanwise centre in the test section. The coordinate system is such that the x- and z-axes are measured from the cylinder axis in the streamwise and spanwise directions respectively, while the y-axis is measured from the lower wall. A hot-wire probe was fixed at an observation station and traversed in the y- and z-directions only. To cover the range of x/d from 2 to 29 the cylinder was moved upstream relative

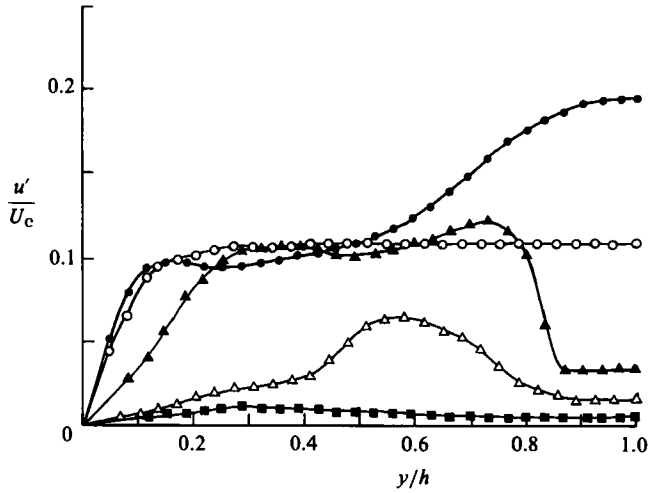

FIGURE 2. Cylinder-generated disturbance introduced into the parabolic flow at $R = 900$: y-distributions of r.m.s. value u' at a streamwise station $x/d = 4$ and at various spanwise positions z/d. The value of U_c for undisturbed parabolic flow is used as a scale for u'. ○, $z/d = 0$; ●, 0.5; ▲, 1.0; △, 1.5; ■, 2.0.

to the hot wire; d denotes the cylinder diameter (10 mm). Another hot wire was transversed in the same manner at the channel exit, $x/d = 160$.

Figure 2 displays y-distributions of u-fluctuations (r.m.s. value u' scaled with U_c) measured at various spanwise positions at $x/d = 4$. The distribution at $z/d = 0.5$ shows a local maximum of about 20 % at the channel centre. This maximum is due to Kármán-vortex-like structures. Indeed the u-fluctuations were quite regular at the channel centre. Even near the wall, the fluctuations exceed 10 %, suggesting the existence of some wall structures: The horseshoe vortices mentioned may break down into hairpin-shaped eddies. This inference is not inconsistent with the distributions at $z/d = 1$, 1.5 and 2.0. As can be seen from the figure, the spanwise extent of the disturbance is more than $2d$ on both sides.

At various x/d stations we traversed the hot-wire probe along three selected y/h = constant lines and determined the maximum u-fluctuation u'_{zm} for each z-distribution. The maximum intensity u'_{zm}/U_c thus determined is plotted against x/d in figure 3 to illustrate the streamwise development of the cylinder-generated disturbance. It grows rapidly immediately behind the cylinder and attains local maxima of 11, 13.5 and 19.5 % for $y/h = 0.3$, 0.6 and 1.0 respectively. The rapid growth is associated with the formation of Kármán-vortex-like structures. Near the wall ($y/h = 0.3$) the intensity remains almost constant at 9–10 % over a considerable streamwise distance. This near-equilibrium is probably due to wall structures like hairpin eddies inferred above. Ultimately, however, the cylinder-generated disturbance decays downstream. Thus at $R = 900$ the disturbed flow is slowly and steadily returning to the original laminar state.

Figure 4 shows oscilloscope traces of typical u-fluctuations observed at $R = 980$ and 1300. Each picture compares the fluctuations at $(x/d, y/d) = (29, 0.3$; upper trace) and (160, 0.6; lower trace). At $R = 980$ the fluctuation is rich in spectral content at $x/d = 29$, but only low-frequency components can survive at the channel exit, $x/d = 160$. The low-frequency components decay slowly, as can be seen from figure 3. On the other hand, at $R = 1300$ we see irregular high-frequency bursts

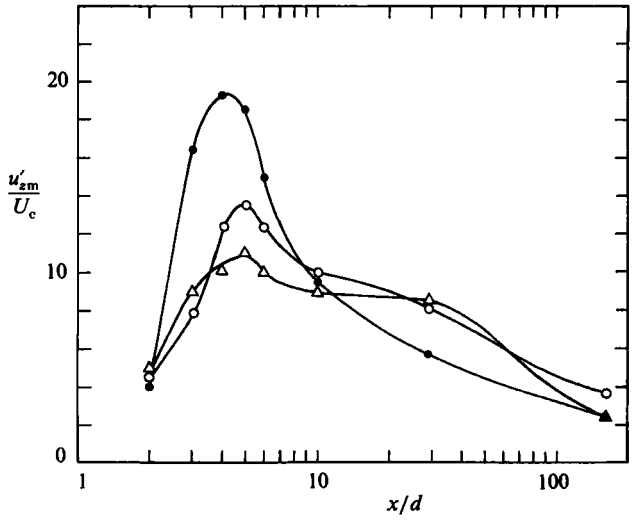

FIGURE 3. Streamwise development of cylinder-generated disturbance: u'_{zm} is the maximum value in the spanwise distribution of u' along y/h = constant line. The value of U_c for undisturbed flow is used as a scale for u'_{zm}. △, $y/h = 0.3$; ○, 0.6; ●, 1.0.

even at the exit. The bursts are the evidence of turbulent-energy production. It is important to note that the bursts did not occur at the exit until R exceeded 1010.

After taking out the cylinder in the test section, we placed six cylinders of the same diameter in the same manner at the channel inlet, at an equal interval of 70 mm in the spanwise direction. We did not measure the disturbance immediately behind the cylinders. But there is little doubt that each cylinder introduced almost the same vortical structures mentioned above. To examine the transition under the highly disturbed inlet conditions, we carefully observed the mean and fluctuation velocities at a downstream distance $650h$ from the inlet, at various Reynolds numbers. Before describing the results, we would like to introduce another Reynolds number R_L defined as $1.5\overline{U}h/\nu$, where $\overline{U}h$ is the volume flow across the half-depth. It should be noted that U_c always stands for the centreline velocity of actual flow (laminar, transitional or fully turbulent), while $1.5\overline{U}$ stands for that of the original parabolic flow before undergoing the transition. Thus R depends on the flow regime, while R_L is unique for a given flow rate and equal to the value of R for the original parabolic flow.

We measured the y-distributions of mean velocity in the range of R_L from 760 to 6400. Figure 5 shows a part of the results to illustrate the transition; related results will be given in §4. At $R_L = 1010$ the flow was intermittently turbulent, with abrupt appearance of high-frequency bursts similar to those shown in figure 4. The bursts may be ascribed to turbulent spots (or patches) visualized by Carlson *et al.* (1982). The intermittency factor roughly estimated is as low as 0.3, and the mean velocity does not noticeably deviate from the parabolic, as seen in the figure. The intermittency increases with increasing R_L, and the flow can be judged to be continuously turbulent beyond $R_L \approx 1600$. However, the mean velocity does not follow the logarithmic law

$$\frac{U}{u_\tau} = A \log\frac{u_\tau y}{\nu} + B.$$

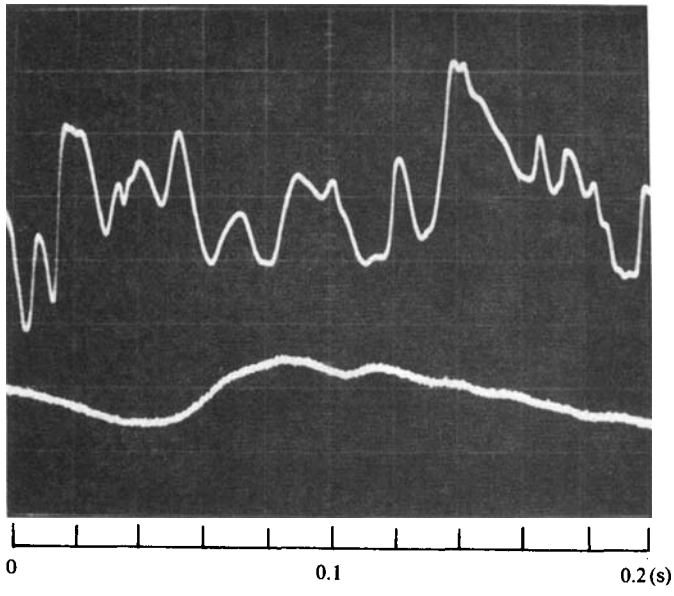

(*a*) $R = 980$

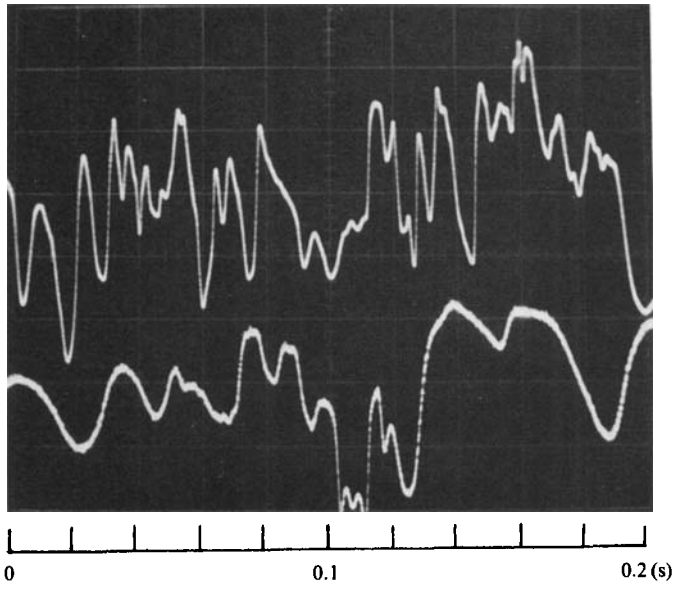

(*b*) $R = 1300$

FIGURE 4. Typical u-fluctuations at $R = 980$ and 1300: these Reynolds numbers are for the undisturbed parabolic flow.

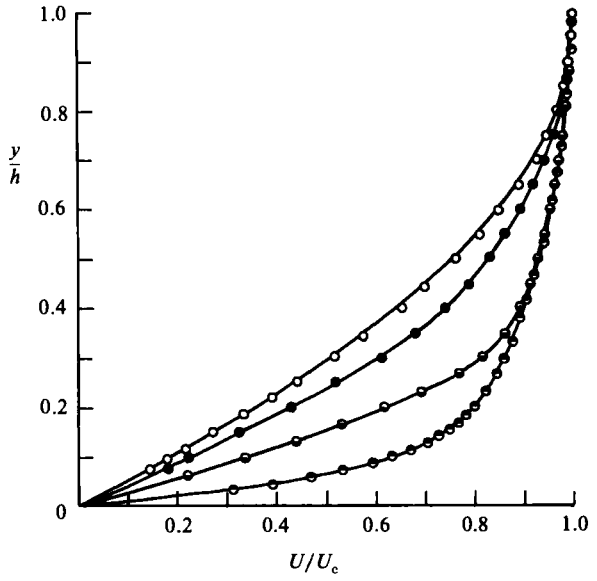

FIGURE 5. Mean-velocity distributions at four Reynolds numbers selected to illustrate the subcritical transition. ○, $R_L = 1010$; ●, 1150; ◒, 1600; ◓, 3950.

It is beyond $R_L = 2000$ that the mean velocity partly follows the log-law distribution, though the constants A and B change with R_L. For instance,

$$(A, B) = \begin{cases} (6.1, 5.9) & \text{at } R_L = 2900, \\ (5.6, 5.5) & \text{at } R_L = 3950. \end{cases}$$

The friction velocity u_τ was estimated from the velocity gradient at the wall.

The relation between R_L and R is shown in figure 6. Data calculated (by the present authors) from Patel & Head's (1969) measurements are also included for comparison. At about $R_L = 1000$ experimental points deviate from the broken line for the parabolic flow. Below $R_L = 1000$ the flow in the test section is almost completely two-dimensional, laminar and parabolic. We observed no remnants of the artificial disturbance due to the six cylinders at the inlet, nor any appreciable distortion in the parabolic flow as far as we could measure in the test section. As noted earlier, the cylinder-generated disturbances is of high intensity, namely 10–20 % depending on the types of vortical structure. These values are comparable to or greater than the maximum intensities of 13–15 % in fully turbulent channel flows above $R_L = 1600$. So we learned that such large disturbances damp ultimately below $R_L = 1000$. We may say that the parabolic flow is totally dominated by viscosity below $R_L = 1000$; in other words, turbulence cannot be self-sustained because of the viscous diffusion and dissipation for Reynolds numbers below 1000.

As described so far, we introduced cylinder-generated vortical disturbances into our low-turbulence wind channel to observe the subcritical transition. The parabolic flow (in the test section) as well as the inlet flow was disturbed. In both cases we found the minimum transition Reynolds number to be about 1000. The disturbances triggering the transition were of 10–20 % intensity, depending on the types of vortical structure; note that this statement does not mean that we could pinpoint the disturbance directly triggering the transition. As noted in §1, however, the observation by Carlson *et al.* suggests the possibility that the disturbance intensity

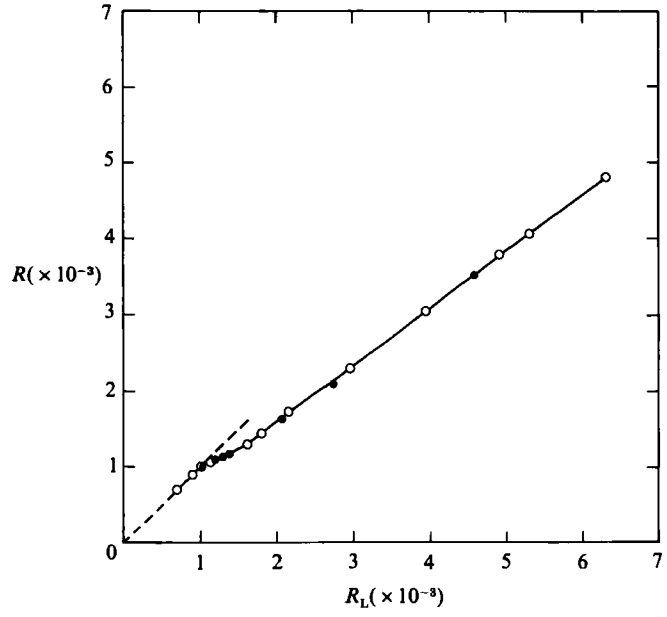

FIGURE 6. Relation between R_L and R. Solid circles, results of Patel & Head; open circles, present results; broken line, parabolic flow.

need not be so large. To check this possibility completely is not easy, because the transition depends on both the type and the intensity of the external disturbance, and it is almost impossible to test all the possible disturbances experimentally. What we could try in order to get some information on this point is to disturb the parabolic flow by means of a periodic jet from a wall orifice of diameter 2.7 mm. The jet was driven by a loudspeaker so that the frequency and the intensity were easily controlled. As the oscilloscope trace of u-fluctuation at $(R, x/d, y/d) = (1300, 160, 0.6)$ in figure 4 shows, the high-frequency bursts occur in association with u-fluctuations of 30–50 Hz. So we drove the jet at 30 and 50 Hz. As a measure of disturbance intensity we took the maximum r.m.s. intensity u'_{jm} at a downstream distance about $2h$ from the orifice. As mentioned before, we took out the hot-wire probe after calibrating the relation between the input to the loudspeaker and u'_{jm}. To judge the transition we observed u-fluctuations at the channel exit (more than $200h$ downstream from the orifice). The appearance of turbulence at the exit showed such on–off character that no remnant of the artificial disturbance could survive when u'_{jm} was below a threshold. Even above the threshold we could see only low-frequency fluctuations below $R_L = 1000$. The low-frequency fluctuations are probably the remnants of structures similar to those that Carlson *et al.* called 'semideveloped spots'. Slightly above $R_L = 1000$, the high-frequency bursts appeared intermittently. The threshold values of u'_{jm}/U_c were 17 and 14 % for jet frequencies 30 and 50 Hz respectively. These values are comparable to those of the cylinder-generated vortical disturbances or to the maximum intensity in fully turbulent channel flows.

4. Concluding remarks

We have described observations of the subcritical transition in plane Poiseuille flow generated in a long wind channel of rectangular cross-section of aspect ratio 27.4. Cylinder-generated vortical disturbances were introduced into the parabolic flow (in

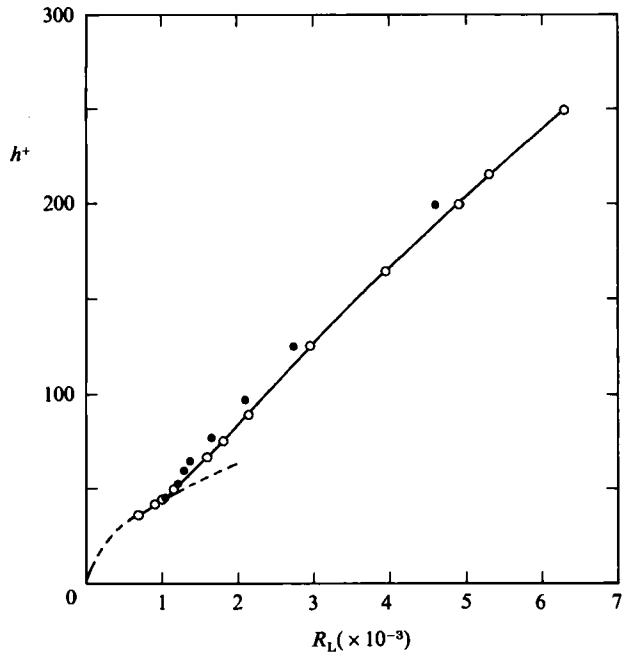

FIGURE 7. Non-dimensional half-depth h^+ (scaled with wall unit) against R_L. Solid circles, results of Patel & Head; open circles, present results; broken line, parabolic flow.

the test section) or the inlet flow. The parabolic flow was also disturbed by a controlled periodic jet from a small wall orifice. The flow was judged to be transitional when bursts of irregular high-frequency u-fluctuations occurred far downstream (from the disturbance generator) because the bursts are sure evidence of turbulent-energy production. From the three kinds of observations we come to the conclusion that the minimum transition Reynolds number is about 1000, and the related threshold intensity (of the external disturbance triggering the transition) is comparable to the maximum intensity of u-fluctuations in fully turbulent channel flows.

The so-called vortex-stretching and tilting effects tend to make the flow three-dimensional and to generate internal thin shear layers. If the shear layers are really formed, they will soon evolve into smaller-scale eddies, resulting in generation of turbulence. Actually these effects are counteracted by the viscous-diffusion and dissipation effects, and thus depend on the Reynolds number. Below $R_L = 1000$ the flow was judged to be dominated by the viscous effects. Indeed, when six cylinders were placed at the inlet, the inlet flow had more than 100% three-dimensional distortions in the mean velocity field because of the reversed flow immediately behind the cylinders, and these distortions disappeared completely far downstream below $R_L = 1000$.

Figure 7 plots the non-dimensional half-depth h^+ (scaled with the wall unit ν/u_τ) against R_L. The broken line is for the laminar parabolic flow. The solid circles represent results calculated (by the present authors) from Patel & Head's data and compared with our results. Let us recall that the flow could be continuously turbulent above $R_L = 1600$ and the mean velocity began to follow the log law at $R_L = 2000$. The figure shows that h^+ is roughly 50, 70 and 90 at $R_L = 1000$, 1600 and 2000 respectively. These values are comparable to the smallest spanwise scales of coherent structures in wall turbulence. Considering these facts, it may be said that any

turbulence structures in the channel, namely even large scales, cannot be free from the viscous effects, in particular below $R_L = 1600$.

The conclusion concerning the threshold mentioned above should be taken as a tentative one, because we could not pinpoint the disturbance directly triggering the transition; namely we could not make clear the type of disturbance that evolved into turbulent spots or patches. To do this, we shall have to study the initial stage of development of the spots in more detail.

The authors wish to express their sincere gratitude to Professors S. Iida, I. Tani and H. Sato for their continual encouragement. This work was partly supported by Grant-in-Aid for Special Project Research 57109004, The Ministry of Education, Science and Culture, Japan. We also wish to thank the referees for helpful comments.

REFERENCES

CARLSON, D. R., WIDNALL, S. E. & PEETERS, M. F. 1982 A flow-visualization study of transition in plane Poiseuille flow. *J. Fluid Mech.* **121**, 487–505.

DAVIES, S. J. & WHITE, C. M. 1928 An experimental study of the flow of water pipes of rectangular section. *Proc. R. Soc. Lond.* A **119**, 92–107.

DIPRIMA, R. C. & STUART, J. T. 1983 Hydrodynamic stability. *Trans. ASME* E: *J. Appl. Mech.* **50**, 983–991.

HERBERT, T. 1976 Periodic secondary motions in a plane channel. In *Proc. 5th Intl Conf. on Numerical Methods in Fluid Dynamics* (ed. A. I. Van de Vooren & P. J. Zandbergen). Lecture Notes in Physics, vol. 59, pp. 235–240. Springer.

HERBERT, T. 1981 Stability of plane Poiseuille flow – Theory and experiment. *Dept. Engng Sci. Mech., Virginia Poly. and State Univ., Rep.* VPI-E-81-35.

HERBERT, T. 1983 Modes of secondary instability in plane Poiseuille flow. In *Proc. IUTAM Symp. on Turbulence and Chaotic Phenomena in Fluids, 1983, Kyoto, Japan.*

KOZLOV, V. V. & RAMAZANOV, M. P. 1980 Experimental investigation of the growth process of disturbances in plane Poiseuille flow. *Preprint* 21, *Inst. Theor. Appl. Mech., AN SSSR SO, Novosibirsk.*

MEKSYN, D. & STUART, J. T. 1951 Stability of viscous motion between parallel planes for finite disturbances. *Proc. R. Soc. Lond.* A **208**, 517–526.

MORKOVIN, M. V. 1983 Understanding transition to turbulence in shear layers. *Dept Mech. Aerosp. Engng, Illinois Inst. Tech., Chicago, Rep.* AFOSR-FR-83.

NISHIOKA, M., ASAI, M. & IIDA, S. 1980 An experimental investigation of secondary instability. In *Proc. IUTAM Symp. on Laminar–Turbulent Transition* (ed. R. Eppler & H. Fasel), pp. 37–46. Springer.

NISHIOKA, M., IIDA, S. & ICHIKAWA, Y. 1975 An experimental investigation of the stability of plane Poiseuille flow. *J. Fluid Mech.* **72**, 731–751.

ORSZAG, S. A. 1971 Accurate solution of the Orr–Sommerfeld equation. *J. Fluid Mech.* **50**, 689–703.

ORSZAG, S. A. & PATERA, A. T. 1983 Secondary instability of wall-bounded shear flows. *J. Fluid Mech.* **128**, 347–385.

PATEL, V. C. & HEAD, M. R. 1969 Some observations in skin friction and velocity profiles in fully developed pipe and channel flows. *J. Fluid Mech.* **38**, 181–201.

STUART, J. T. 1960 On the non-linear mechanics of wave disturbances in stable and unstable parallel flows. Part 1. *J. Fluid Mech.* **9**, 353–370.

ZAHN, J.-P., TOOMRE, J., SPIEGEL, E. A. & GOUGH, D. O. 1974 Non-linear cellular motion in plane Poiseuille flow. *J. Fluid Mech.* **64**, 319–345.